

NATURAL CONVECTIVE FLOW IN A MULTILAYERED VERTICAL POROUS MEDIA

مريان الحمل الطبيعي في وسط مسامي رأسي متعدد الطبقات

M. S. EL KADY

Mechanical Engineering Department  
Mansoura University, Egypt

خلاصه:

يبين هذا البحث دراسه عدديه للحمل الطبيعي الحر في حيز تنقي البعد في شكل متعامد مملوه بوسط مسامي متعدد الطبقات الراسيه ومعرض لفرق في درجات الحراره بين الجدارين الراسيين. وقد تركزت هذه الدراسه على تأثير عدم تماوى درجه النفاذيه للطبقات الراسيه ونسبه البعد للطبقة الوسطى لوسط ثلاثى الطبقات الراسيه على سلوك كل من درجات الحراره وسرعه المتع وخطوط مريان المتع وكذلك على الاماظ المختلفه لانتقال الحراره. الطبقة الاولى والثالثه لهما نفس العرض ودرجه النفاذيه بينما يتراوح مدى التغير في درجه النفاذيه للطبقة الوسطى بالنسبه الى درجات النفاذيه للطبقات الاخرى Kr من 0.1 الى 10 ونسبه بعدها الى العرض الكلى Wr من صفر الى 1.0. وقد حلت كل من معادلات اللاسمرار وكميه الحركه والطاقه عدديا باستخدام طريقه الفروق البسيطه. كما اجريت مقارنات للنتائج مع النتائج التي حصل عليها لوريك وبراند (12) لظهور تطابقا جيدا وثبتت صحه هذا النموذج. وقد اظهرت النتائج حاصليه شكل المريان والسرعه ودرجات الحراره داخل الوسط المسامي للتغير في درجه النفاذيه. ومن النتائج تبين ايضا ان خواص انتقال الحراره تعتمد على كل من Kr, Wr وذلك بالاضافه الى الاعتماد المعروف مسبقا على نسبة الاطوال (الارتفاع/العرض) وعدد ريلى. وقد اظهرت الزيادة في عدد ريلى ثلاثة اమాظ مختلفه لانتقال الحراره وهى التوصيل، انتقالى، ونمط انتقال الحراره خلال الطبقة العديه. كما استنتجت علاقه عدديه تعبر عن تأثير كل من نسبة درجه النفاذيه ونسبه البعد للطبقة الوسطى على عدد نوميك وذلك في نمط انتقال الحراره من خلال الطبقة العديه في الحالة المدروسه كما يلي:

$$Nu = C \cdot (\pm 0.3836 Wr + 1) (0.0454 Kr + 0.9546) \cdot Ra^{0.7}$$

العلامه الموجبه عندما تكون  $Kr > 1$  والعلامه السالبه في حاله  $Kr < 1$  والثابت C يعطى على نسبة الابعاد

ABSTRACT

Convective heat transfer through a vertically multilayered porous media is examined numerically. The examination is focused upon the effect of the nonuniform permeabilities of the sublayers on the behavior of the temperature, flow fields and the different regimes of the heat flow. The study was done on a model with vertical isothermal walls at different temperatures and horizontally perfect insulated walls, and for three layered porous medium in which the first and third layers have equal thicknesses and permeabilities. The numerical results are reported for a range of the permeability ratio of the inner sublayer  $0.1 < Kr < 10$  and a range of the width ratio of the inner sub-layer to the total width  $0.0 < Wr < 1.0$ ,  $0 < Ra < 5000$  and for an Aspect ratio  $A=3$ . The governing equations are written in terms of nondimensional variables and solved using the finite difference method. A

comparison is made with the results obtained by Lauriat and Prasad [12]. The comparison shows a very good agreement for the presented results and proves the validity of the model. The results give a very good idea about the effect of the inhomogeneity of the porous medium on the flow structure and temperatures. It is found also that the heat transfer characteristics depend on both  $K_r$  and  $W_r$  besides the known dependence on the  $Ra$  and the aspect ratio. Three regimes of heat flow is obtained by increasing of Rayleigh number, Conduction, transient and boundary layer regime. A numerical correlation expresses the effect of both  $W_r$  and  $K_r$  on  $Nu$  is derived for the boundary layer regime for this particular case as follows:

$$Nu = C \cdot (+0.3836 W_r + 1)(0.0454 K_r + 0.9546) Ra^{0.5}$$

where the +ve is for the case of  $K_r > 1$ , the -ve is for the case of  $K_r < 1$  and  $C$  is constant depends on the Aspect ratio.

## 1. INTRODUCTION

The heat transfer by natural convection across a porous medium heated from one side is a topic of fundamental importance in diverse fields such as thermal insulation engineering, geothermal reservoir dynamics and grain storage. The basic model used so far in the study of porous media heated from one side consists of a 2-dimensional layer with vertical isothermal walls at different temperatures and with adiabatic top and bottom walls. This model has been investigated extensively during the past 20 years. The first study of the problem, an experimental one, was reported by Schneider [1]. He investigated the natural convection heat transfer through granular material under the condition of fixed height and width. The first extensive theoretical work on this problem was performed by Chan et al. [2]. Later on, these studies were followed by a number of investigations, out of which the notable theoretical solutions presented in [3-13]. Weber [3] reports an Oseen-linearized analysis of the boundary layer regime in a tall layer; Weber's analysis was improved by Bejan [4] to account for the heat transfer vertically through the core and, in this way, to predict correctly the heat transfer rates revealed by experiments and by numerical simulations. Simpkins and Blythe [5] reported an alternative theory for the boundary layer regime based on an original closed form solution, and for temperature dependent viscosity [6]. The corresponding flow in the shallow layer heated from the sides was documented by Walker and Homsy [7]. They developed an asymptotic solution for the flow and temperature fields inside a shallow layer using the aspect ratio as the small parameter. They showed that unlike the in the tall layers the core region plays an active role in the heat transfer processes. An approximate integral type solution for the same geometry was reported by Bejan and Ilen [8]. Tong and Subramanian [9] have presented a boundary layer analysis for a Brinkman model, and have reported significant contributions of the diffusion term at high Rayleigh and Darcy numbers. Furthermore, Poulikakos and Bejan [10] and Prasad and Tuntomo [11] have considered the

Forchheimer-extended Darcy model to study the inertia effects on free convection in a vertical cavity. Lauriat and Prasad [12] considered the Brinkman-extended Darcy equation of motion together with the transport term and examined the significance of each term. Elkady [13] clarified numerically the effect of the dimensions of the rectangular cavity on the heat transfer through an inclined cavity with variable inclination angles from 0 to 180.

The survived literature presented above have been concerned with natural convection in layers only filled with homogeneous porous medium, which may not be a good approximation for the porous layers in the real life. The purpose of this study is to analyse and understand the effect of the inhomogeneity of the porous medium on the flow structure and the convective heat transfer in a vertically layered porous media with vertical isothermal walls at different temperatures.

## 2. MATHEMATICAL MODEL AND SOLUTION PROCEDURE

Consider a two-dimensional rectangular vertical cavity (shown in Fig. 1) of width  $W$  and height  $H$ , filled with multilayered porous medium. Each layer is homogeneous, isotropic and has constant permeability  $K$ . The porous medium is saturated with a single phase fluid of density  $\rho$  and viscosity  $\mu$ . In Fig.1  $T_H$  and  $T_c$  represent the hot and cold vertical walls of the cavity respectively, while the horizontal top and bottom walls are insulated. The effect of both the drag and inertia are neglected, and the flow will obey Darcy's law.

The fluid properties are assumed to be constant except for the density change with temperature which gives rise to the buoyancy force, this is treated by invoking the Boussinesq approximation. While the permeability values  $K$  of the porous layers are different, the values of the thermal diffusivity in the layers are the same. This assumption is done to study the effects of the change of the permeability alone. With these assumptions, the conservation equations for the mass, momentum and energy for each layer become:

Continuity

$$\partial u / \partial x + \partial v / \partial y = 0 \quad (1)$$

Momentum (Darcy's law)

$$\partial p / \partial x + (\mu / K) u = 0 \quad (2)$$

$$\partial p / \partial y + (\mu / K) v = \rho g \beta (T - T_c) \quad (3)$$

Energy

$$u \partial T / \partial x + v \partial T / \partial y = \alpha (\partial^2 T / \partial x^2 + \partial^2 T / \partial y^2) \quad (4)$$

where  $u$ ,  $v$ ,  $p$ ,  $\alpha$ ,  $\beta$ ,  $g$ ,  $\mu$  and  $K$  are the velocity components in the  $x$  and  $y$  directions, pressure, thermal diffusivity, coefficient of thermal expansion, acceleration due to gravity, kinematic viscosity and permeability of the porous media, respectively.

Eliminating the pressure terms from equations (2) and (3), introducing the stream function  $\psi$  as  $u = \partial\psi/\partial y$  and  $v = -\partial\psi/\partial x$  and scaling all the variables by appropriate characteristic values of those variables defined by:

$X = x/W$ ,  $Y = y/H$ ,  $\psi = \rho H/\alpha W$ , and  $\theta = (T-T_c)/(T_h-T_c)$  the governing equations (1)-(4) can be transformed into a non-dimensional stream function and a temperature equations

$$\nabla^2 \psi / A^2 + (1/A^2) \nabla^2 \psi = -Ra (\partial\theta/\partial X) \quad (5)$$

$$U \partial\theta/\partial X + V \partial\theta/\partial Y = A^2 (\partial^2\theta/\partial X^2 + \partial^2\theta/\partial Y^2) \quad (6)$$

where  $A$  is the aspect ratio of the cavity  $= H/W$  and  $Ra$  is the Darcy-Rayleigh number based on the height of the cavity  $H$ , and is given by

$$Ra = Kg\beta(T_h - T_c)H/\alpha\nu$$

Because the vertical layers have different permeabilities  $K$ , the Darcy-Rayleigh number  $Ra$  will be different for each layer. Taking the permeability ratio for each layer as  $K_r = K/K_h$ , the Darcy-Rayleigh number for each layer will be:

$$Ra = K_r Ra_h$$

where  $K_h$ ,  $Ra_h$  are taken as the permeability and the Darcy-Rayleigh number in the layer in contact with the hot wall.

The boundary conditions for the nondimensional stream function and temperature are as follows:

$$\psi = 0 \text{ on all walls, } \partial\theta/\partial Y = 0 \text{ for } Y=0,1 \text{ and } 0 < X < 1,$$

$$\theta = 1 \text{ for } X=0 \text{ and } 0 \leq Y \leq 1, \theta = 0 \text{ for } X=1 \text{ and } 0 < Y < 1.$$

The effect of the fluid motion on the heat transfer across the layers can be expressed by the Nusselt number, which is defined for the vertical hot wall in the non dimensional form as:

$$Nu = \int_0^1 Nu_y \Big|_{x=0} dy \quad (7)$$

$$\text{and } Nu_y = - \frac{\partial\theta}{\partial X}$$

where  $Nu$  is the average (mean) Nusselt number at the wall  
 $Nu_y$  is the local Nusselt number

The solution of the governing differential equations (5) and (6) has been obtained numerically by using the finite difference scheme presented by Patankar [16]. The solution consists of the stream function and the temperature fields as well as the velocities in the  $x$  and  $y$  directions. More detailed information about the numerical procedure is presented in [14]. After obtaining the temperature field, equation (7) was integrated numerically to get the  $Nu$ .

### 3. RESULTS AND DISCUSSION

The two dimensional natural convection in a multilayered with different permeabilities fluid saturated porous medium has been

analyzed for vertical isothermal walls at different temperatures and with adiabatic top and bottom walls. The study is made for three layered porous medium in which the first and third layers have equal thicknesses and permeabilities. The permeability ratio  $K_r$  of the inner sublayer varies from 0.1 to 10 and the width ratio of the inner sub-layer  $W_r$  varies from 0.0 to 1.0 for a wide range of Darcy-Rayleigh number up to 6000.

### 3.1 The validity of the model

In the following study in sections 3.2 and 3.3, the cases of  $W_r = 0.0$  and 1.0 are corresponding to those cases of a uniformly filled cavity, and the results obtained for these cases are in good agreement with those obtained by the author in previous study [13].

Another comparison is done with the results obtained by Lauriat and Prasad [12] for a case of a single layer porous media with  $W_r = 0$ ,  $A = 5$ . The values of the vertical velocity  $V/Ra$  and the temperature  $\theta$  at the midheight section where  $Y = 0.5$ , the horizontal velocity  $U/Ra$  at  $X = 0.5$  for  $Ra = 250, 1000$  and  $2500$ , the local  $Nu$  at  $Ra = 2500$  and the average  $Nu$  at the hot wall at  $0 < Ra < 6000$  of Lauriat and Prasad [12] are translated into the corresponding notations and expressions by this work and compared with it. The comparison which is shown in Figs 2-5 shows a very good agreement and proves the validity of the model.

A relation similar to equation (7) for the heat flow along the cold wall  $x = W$ ,  $X = 1$  was obtained and integrated numerically. The obtained  $Nu$  was compared with this calculated from equation (7). The results were found to be nearly identical, the discrepancy between the results of the two approaches was less than 0.75%.

## 3.2 TEMPERATURE AND FLOW FIELDS

### 3.2.1 Effect of sublayers width

Figs. 8-12 show the effect of the width ratio of the inner sublayer  $W_r$  on the streamlines and isothermal lines. The width ratio  $W_r$  takes the values 0.0, 0.2, 0.4, 0.6, 0.8, 1.0.

Figs 6-9 show the case where the permeability of the inner layer is five times greater than the outer layers  $K_r = 5$ , the aspect ratio  $A = 3$  and  $Ra = 150$ . In the case of  $W_r = 0.0$ , where the whole cavity is filled with low permeability porous media, the streamlines shown in Fig. 6, tend to be in the outer region of the sublayers with less flow in the core. With the appearance of the higher permeability inner sublayer, an attraction appears for the flow towards the core, and the tendency for more flow to be initiated in this attractive layer exists. With the increase of  $W_r$  the attraction for the flow towards the core increases, and higher values of streamfunction exists also, carrying more convective heat from the hotter side to the colder one. The flow

rate increases with the increase of  $Wr$ , and the slope of the axis of the cells changes significantly. For example at  $Wr=0$ , the axis is close to the vertical middle plane, but with the increase of  $Wr$ , the axis moves towards the diagonal of the cavity. Therefore, the maximum velocities (horizontal and vertical components) drift from the vertical and horizontal middle planes to the corners (left bottom and right top corners).

An indication for the transport of energy by convection between the two isothermal vertical walls is the rate of flow inside the cavity, which can be expressed by the maximum value of the streamfunction and the mean velocity of the flow. To express these two functions two variables are used in [13-15], and are defined as:

$$\psi_{max} = \pm \max |\psi(x,y)| \quad \text{and} \quad U_m = \frac{1}{A} \int (U^2 + V^2) dA$$

where  $\psi_{max}$  is the maximum value of the non-dimensional streamfunction.  $\pm$  are taken for counter clockwise and clockwise circulation respectively and  $U_m$  is expressed as a function of the average fluid speed over the area  $A$ .

Fig. 7 shows the behavior of the functions expressed by  $U_m/U_{m0}$  and  $\psi_{max}/\psi_{max0}$  with the increase of  $Wr$ , where  $U_{m0}$  and  $\psi_{max0}$  are the functions in the case of  $Wr=0$ . The figure shows a significant increase of both the two functions with the increase of  $Wr$  indicating the increase of the transport energy by convection part in the whole layers.

The behavior of the isothermal lines for different inner sublayer width ratios  $Wr$  is shown in Fig. 8. It is noticed that the interior temperature distribution is close to a straight line in the central part of the inner sublayer. The slope of these isothermal lines shows that the heat is transferred by both conduction and convection. With the increase of the width of the attractive inner sublayer, the isothermal lines in the inner sublayer deviate towards the horizontal direction (normal to the walls of the heat flow), indicating the increase of the transport of energy by convection part in the core region. The temperature gradients near the bottom left and the right top corners are greatly modified to a sharp temperature gradients. Thus the transport of energy due to cross flow near the horizontal walls has also increased.

Fig. 9 shows the effect of the inner sublayer width ratio  $Wr$  on both the temperature and velocity distributions at the middle height of the porous media  $Y=0.5$  in the half of the width adjacent to the hotter side. For the case of  $Wr=0$ , where the whole cavity is filled with low permeability porous media, both the temperature and velocity distribution curves are nearly straight lines. With the increase of  $Wr$  both the temperature and velocity curves deviate from the straight line condition in the inner sublayer and remain taking the nearly straight line shape in the lower permeability outer layer near the hotter side, with

a significant increase in the velocity field and decreasing temperatures. The step variation in the permeability across the interface of the two sublayers induces step changes in the slopes of both velocities and temperatures. The break points in both fields are shown by the symbole (o).

Figs. 10-12 show another case, where the permeability of the inner layer is five times less than it in the outer layers, i.e.  $K_r$  for the inner sublayer = 0.2, the aspect ratio  $A=3$  and  $Ra=400$ . The behavior of the streamlines for different values of  $W_r$  is shown in Fig. 10. For the case of uniform porous media where  $W_r=0.0$ , i.e. high permeability layer, the temperature difference across the two vertical walls causes a relatively high velocity flow all over the layer. As the less permeability inner sublayer appears, A new resistance appears for the flow in the core of the inner sublayer. With the increase of  $W_r$ , the damping for the existing flow in the core increases. The slope of the axis of the cells changes significantly. AT  $W_r=0$  the axis is close to the diagonal of the cavity, but with the increase of  $W_r$ , the axis moves towards the vertical middle plane indicating that the maximum velocities (horizontal and vertical components) drift from the corners (left bottom and right top corners) to the vertical and horizontal middle planes. Therefore, the flow is attracted to be vertically in the outer layers, where the higher permeability exists, and is forced to be exchanged between the outer sublayers carrying the convective heat energy part through the upper and lower ends of the inner layer, and less flow of convective energy transfer through the core region.

Fig. 11 shows the behavior of the functions  $U_m/U_{m0}$  and  $\psi_{max}/\psi_{max0}$  with the increase of  $W_r$ . The figure shows a significant decrease of both the two functions. This indicates the decrease of both the mean velocity of the flow and the rate of flow inside the cavity, which in turns decreases the transport energy by convection part in the whole layers.

Fig. 12 shows the behavior of the isothermal lines for different values of  $W_r$ . In the core of the inner sublayer, where, less flow exists, the above modification in the velocity field with the increase of  $W_r$  changes the isotherm pattern accordingly. The isothermal lines deviate towards the vertical direction (parallel to the isothermal walls) indicating the decrease of convection heat flow through the core region. The sharp temperature gradients near the bottom left and the right top corners are greatly modified, and the transport of energy due to the cross flow near the horizontal walls has, thus, decreased.

### 3.2.2 Effect of permeability ratio

Figs. 13-15 show the streamlines and the isothermal lines behavior for three layers porous media with equal widths,  $Ra=250$ , Aspect ratio = 3 and different permeability ratios for the inner to the outer sublayers  $K_r$  from 10 to 0.1.

The behavior of the streamlines for different values of  $K_r$  is shown in Fig. 13. For the case of high permeability uniform porous media where  $K_r=1$ , the temperature difference across the two vertical walls causes a relatively high velocity flow all over the layer. For the case of  $K_r>1$ , with the increase of  $K_r$ , the attraction for the outer streamlines to change its direction gradually towards the core of the inner sublayer increases, besides the increase of the chance for the fluid rate of flow in the core to increase, carrying more convective heat from the hotter side to the colder one. For the case of  $K_r<1$ , with the decrease of the permeability ratio  $K_r$ , the streamlines find an increased resistance to flow in the core of the inner sublayer, and is forced to change its direction gradually and compressed in the outer sublayers, tending to be parallel to the outer vertical walls. The flow is forced to be exchanged between the outer sublayers through the upper and lower ends of the inner sublayer.

This phenomenon reflects itself on the maximum value of the stream function and the mean velocity of the flow in the cavity. Fig. 14 shows the increase of both  $U_m/U_{m1}$  and  $\psi_{max}/\psi_{max1}$  with the increase of the permeability ratio of the inner sublayer.

Fig. 15 shows the behavior of the isothermal lines for different values of  $K_r$ . With the decrease of the inner sublayer permeability ratio  $K_r$  the above modification in the velocity field changes the isotherm pattern accordingly. The isothermal lines deviate towards the vertical direction (parallel to the isothermal walls) indicating the decrease of convection heat flow through the core region. The sharp temperature gradients near the bottom left and the right top corners are greatly modified, and the transport of energy due to the cross flow near the horizontal walls has, thus, decreased also.

### 3.3 Heat transfer

#### 3.3.1 Effect of permeability ratio

To show the effect of the permeability ratios, a case of three layers porous media with equal widths are studied. In which the aspect ratio  $A = 3$ , the permeability ratios for the inner to the outer sublayers  $K_r$  differ from 10 to 0.1 and  $Ra=250$ .

The behavior of the local rate of heat transfer  $Nu_y$  along the hot wall is shown in Fig. 16. It takes the typical trend as obtained in [12,14], in which the higher values of the rate of heat transfer exist at the bottom of the wall and then it drops to the lower values at the top of the wall. Fig. 18 shows the increase of the rate of local heat transfer with the increase of the inner sublayer permeability ratio.

Fig. 17 shows the effect of the permeability ratio of the inner sublayer on the average rate of heat transfer expressed by  $Nu$  for different  $Ra$ . Fig. 18 shows the variation of  $Nu/Nu_1$  with  $Ra$  for different values of  $K_r$ . Where,  $Nu_1$  is the value of  $Nu$  for



\* the case where the whole cavity is filled with the porous material of the layer adjacent to the hot wall, i.e.  $Kr$  for the inner sublayer=1 or  $Wr=0$ . It is shown that  $Nu/Nu_1$  is greater than 1 for  $Kr>1$  and less than 1 for  $Kr<1$ , i.e.  $Nu$  is higher than its value for a homogenous filled cavity by  $Kr>1$  and less than it by  $Kr<1$ . Both the  $Nu/Nu_1-Ra$  and  $Nu-Ra$  curves take nearly the same form for the different permeability ratio  $Kr$ . In all cases, where  $Ra=0$  at the hot wall,  $Nu/Nu_1$  and  $Nu$  take the unity value and the heat is transferred by pure conduction. By the increase of  $Ra$ ,  $Nu/Nu_1$  increases in a transient region until it takes a parallel straight line form by  $Ra>1000$ , where  $Nu/Nu_1$  depends only on  $Kr$ . The behavior of  $Nu/Nu_1$  is shown in Fig. 19. It gives a linear relation as follows:

$$Nu/Nu_1 = 0.0454 Kr + 0.9546 \quad (8)$$

Kim and Vafia [17] studied the natural convection about a vertical plate embedded in a homogenous porous media. They concluded that the Nusselt number depends only on the Rayleigh number  $Ra$  in the thermal boundary layer, where the heating effect of the wall is felt. This conclusion is also concluded by Weber [3] by studying the boundary layer regime for convection in a vertical homogenous porous layer. The mean value of  $Nu$  for the boundary layer heat flow in the homogenous porous media can be given according to [3,17] in our notations by following relation:

$$Nu = C Ra^A \quad (9)$$

where  $C$  is a constant, which depends on the aspect ratio  $A$ . By Weber [3] this constant is obtained as  $1/(3A)$  for the boundary layer flow. In this case, the heat conducted from the wall into the fluid is carried upwards by the convective movement of the fluid in the steady state, and the fluid is driven upwards by buoyancy and restricted by bulk friction. This means that outside this layer, where the fluid is isothermal and the buoyancy effect is absent the fluid is nearly motionless.

In our case, for the  $Nu/Nu_1$  straight line zone, where  $Ra>1000$ , and  $Nu/Nu_1$  is mainly function of  $Kr$ , it can be said that the heat is transferred in a boundary layer flow. This flow consists of upward boundary layer on the hot wall, downward boundary layer on the cold wall and motionless flow in the core, thus equation (9) can be considered. The constant  $C$  in equation (9) must be dependent on both the permeability ratio  $Kr$  and the width ratio  $Wr$  of the inner sublayer besides the aspect ratio  $A$ . Because the aspect ratio  $A$  and the width ratio  $Wr$  are constants and equation (8) gives that  $Nu/Nu_1=f(Kr)$ , it can be said that the effect of both  $Kr$  and  $Wr$  on  $C$  can be separated, and  $C$  can be written as

$$C = f(Wr) \cdot f(Kr) \cdot f(A) \quad (10)$$

### 3.3. Effect of sublayers width

To show the effect of the sublayers width ratio  $Wr$ , a constant values for the permeability ratios of the sublayers will

be considered. Figs. 20-26 show the effect of the width ratio of the inner sublayer  $W_r$  on the Local and mean  $Nu$  at the vertical hot wall. The width ratio  $W_r$  takes the values 0.0, 0.2, 0.4, 0.6, 0.8, 1.0, for an aspect ratio  $A=3$ . Two cases are considered. In the first case, the permeability of the inner sublayer is taken as five times greater than the outer layers  $K_r=5$  and  $Ra=150$ . In the second case, the permeability of the inner sublayer is taken as five times less than it in the outer layers  $K_r=0.2$  and  $Ra=400$ .

Figs. 20 and 21 show the distribution of the local rate of heat transfer  $Nu_x$  along the hot wall. The Figures show that the rate of local heat transfer increases with the increase of the inner sublayer width ratio for  $K_r > 1$ , and decreases with the increase of the sublayer width for  $K_r < 1$ .

Figures 22 and 23 show the variation of the  $Nu$  for different values of the width ratio for the two cases of study. The behaviour of the  $Nu$ - $Ra$  curve is nearly the same as that expressed in Fig. 17. It consists also from the three zones. The zero  $Ra$  at the hot wall where  $Nu=1$  and the heat transferred by pure conduction, the transient zone and the boundary layer flow zone. It is shown that  $Nu$  increases with the increase of the width ratio  $W_r$  by the case of  $K_r=5$  and  $Nu$  decreases with the increase of the width ratio  $W_r$  by the case of  $K_r=0.2$ .

Figures 24 and 25 show the behavior of the function  $Nu/Nu_1$  for the two expressed cases. It is shown that the value of  $Nu$  is higher than its value for a homogenous filled cavity by  $K_r=5$  and less than it by  $K_r=0.2$ . It is also shown that in the boundary layer flow zone, where  $Ra > 1000$ , the value of  $Nu/Nu_1$  is nearly constant and depends on the width ratio  $W_r$  only. This relation is shown in Fig. 26. It gives a linear relation as follows

$$Nu/Nu_1 = \pm 0.3836 W_r + 1 \quad (11)$$

the +ve is for the case of  $K_r > 1$  and the -ve for  $K_r < 1$

For the general case, equations 8 and 11 can be combined together to give the effect of both the permeability and width ratios in the boundary layer flow regime where  $Ra > 1000$ . It can be expressed as follows:

$$Nu/Nu_1 = (\pm 0.3836 W_r + 1)(0.04342 Kr + 0.952) \quad (12)$$

Equation (9) which expresses the heat transfer in the boundary layer flow regime can be developed to take into consideration the effects of both the permeability ratio  $K_r$  and width ratio  $W_r$  for the three layered porous media and written as:

$$Nu = C (\pm 0.3836 W_r + 1)(0.0454 Kr + 0.9546) Ra^{0.5}$$

where the +ve is for the case of  $K_r > 1$ , the -ve for  $K_r < 1$  and  $C$  depends on the aspect ratio  $A$ .

#### 4. CONCLUSIONS

This paper outlined numerically the phenomenon of the fluid flow by natural convection in a two dimensional vertical multilayered porous medium with different permeabilities and heated from one side. The study is focused on the effect of the non-uniform permeability of the sublayers on the behavior of the temperature, streamlines fields and the heat transfer. The results indicate the following:

With the increase of  $K_r$  or  $W_r$  for  $K_r > 1$  or the decrease of  $W_r$  for  $K_r < 1$ ,

- the slope of the axis of the streamlines cells moves from the vertical middle plane towards the diagonal of the cavity.
- The maximum velocities (horizontal and vertical components) drift from the vertical and horizontal middle planes to the corners (left bottom and right top corners).
- the attraction for the flow towards the core increases, the flow rate and the mean velocity in the cavity increase and higher values of streamfunction exists, carrying more convective heat from the hotter side to the colder one.
- the interior temperature distribution is close to a straight line in the central part of the inner sublayer. The isothermal lines deviate from the vertical direction (parallel to the isothermal walls) towards the horizontal direction (normal to the isothermal walls) indicating the increase of the transport of energy by convection part in the core region.
- The temperature gradient near the bottom left and the right top corners is greatly modified to a sharp temperature gradient, indicating the increase of the transport of energy due to cross flow near the horizontal walls.

With the decrease of  $K_r$  or the increase of  $W_r$  for  $K_r < 1$  or the decrease of  $W_r$  for  $K_r > 1$ , the damping for the existing flow in the core increases, and the flow is attracted to be vertically in the outer layers, where the higher permeability exists, and is forced to be exchanged between the outer sublayers carrying the convective heat energy part through the upper and lower ends of the inner layer.

For a constant width ratio, both the rate of local heat transfer and the mean heat transfer at the hot wall increase with the increase of the inner sublayer permeability ratio and are higher than its values for a homogenous filled cavity by  $K_r > 1$  and less than it by  $K_r < 1$ .

For a constant permeability ratio both the rate of local heat transfer at the hot wall and the mean heat transfer increase with the increase of the inner sublayer width ratio for  $K_r > 1$ , and decrease with the increase of the sublayer width for  $K_r < 1$ .

The behavior of  $Nu$  at the hot wall with the increase of  $Pr$  takes 3 stages:

- $Nu = 1$  and the heat transferred by pure conduction when  $Rah = 0$ .

- transient heat flow by  $0 < Ra_w < 1000$
- boundary layer flow by  $Ra_w > 1000$ . In which the mean rate of heat transfer depends on both the width ratio, the permeability ratio in addition to the dependence on the Rayleigh number and the aspect ratio. A correlation is derived numerically for this relationship as follows:

$$Nu = C \cdot (\pm 0.3838 W_r + 1) (0.0484 Kr + 0.9548) Ra^{0.5}$$

where C is a constant depends of the aspect ratio A, the +ve is for the case of  $Kr > 1$  and the -ve for the case of  $Kr < 1$ .

## 5. NOMENCLATURE

A	Aspect ratio = $H/W$
g	Acceleration due to gravity, $m^2/s$
H	Height of the porous material, m
K	Permeability of the porous layer, $m^2$
$K_H$	Permeability of the porous layer adjacent to the hot wall, $m^2$
$K_r$	Ratio of the permeability of the porous layer to the permeability of the porous layer adjacent to the hot wall = $K/K_H$
p	Pressure, Pa
Ra	Darcy-Rayleigh number = $g \beta K H C (T_H - T_c) / \alpha \nu$
$Ra_w$	Darcy-Rayleigh number for the layer adjacent to the hot wall
T	Temperature, K
$T_H, T_c$	Temperature of the hot and cold isothermal surfaces, K
u, v	Field velocities in the x and y directions, $m/s$
U, V	Non-dimensional field velocities in the X and Y directions respectively
$U_m$	Fluid non-dimensional average velocity
x, y	Spatial coordinates
X, Y	Dimensionless distances in the x and y axis respectively
W	Width of the porous material, m
$W_r$	width ratio
$\alpha$	Thermal diffusivity of the porous layers, $m^2/s$
$\beta$	Coefficient of volumetric thermal expansion, $1/K$
$\mu$	Dynamic viscosity of the fluid
$\nu$	Kinematic viscosity of the fluid, $m^2/s$
$\rho$	Fluid density $kg/m^3$
$\phi$	Stream function
$\psi$	dimensionless stream function
$\psi_{max}$	Maximum extremum value of the stream function
$\theta$	Non-dimensional temperature = $(T - T_c) / (T_H - T_c)$

## 6. REFERENCES

1. Schneider, K. J. "Investigation of the influence of free thermal convection on heat transfer through granular material," Proceedings, International Institute of Refrigeration, pp 247-253, 1963.
2. Chan, B. K. C., Ivey, C. M., and Barry, J. M., "Natural convection in enclosed porous media with rectangular

- boundaries", ASME J. of Heat Transfer, Vol. 2, pp 21-27, 1970
3. Weber, J. E., "The boundary layer regime for convection in a vertical porous layer." Int. Journal of Heat and Mass Transfer, Vol. 18, pp 569-573, 1975.
  4. Bejan, A., "On the boundary layer regime in a vertical enclosure filled with porous medium". Lett. Heat Mass Transfer, Vol. 8, pp 93-102, 1979
  5. Simpkins, P., and Blythe, P., "Convection in a porous layer" Int. Journal Heat Mass Transfer, Vol. 23, pp 881-887, 1980.
  6. Blythe, P. A., and Simpkins, P. g., "Convection in a porous layer for a temperature dependent viscosity", Int. Journal Heat Mass Transfer, Vol. 24, pp 497-506, 1981.
  7. Walker, K. L. and Homsy, G. M., "Convection in a porous cavity" Journal of Fluid Mechanics, Vol. 87, pp 449-474, 1978.
  8. Bejan, A. and Tien, C., "Natural convection in a horizontal porous medium subjected to an end to end temperature difference". J. of heat transfer, Vol. 100, pp 191-198, 1978.
  9. Tong, T, and Subramanian, E., "A boundary layer analysis for natural convection in a porous enclosure - use of the Brinkman extended Darcy model". Int. Journal of Mass and Heat Transfer, Vol. 28, pp 563-571, 1985.
  10. Poulikakos, D., and Bejan, A., "The Departure from Darcy Flow in Natural Convection in a Vertical Porous Layer", Physics of Fluids, vol. 28, pp. 3477-3484, 1985.
  11. Prasad, V., and Tuntoma, A., "Inertia effect on natural convection in a vertical Porous cavity", Numerical Heat Transfer, 1987.
  12. Lauriat, G. and Prasad, V., "Natural convection in a vertical porous cavity: a numerical study for Brinkman-extended Darcy formulation", Trans. of the ASME, Vol 109, pp 688-696, 1987.
  13. El Kady, M.S., "Natural convection in an inclined rectangular porous medium at various angles and aspect ratios", Mansoura Engineering Journal (MEJ), vol 15, No. 2, pp M50-M68, 1990.
  14. El Kady, M.S., "Numerical study of natural convection in a rectangular porous medium with vertical temperature gradient". Man. Eng. Journal (MEJ), vol. 15, No. 1, pp M72-M87, 1990.
  15. El Kady, M.S., "Effect of the Aspect ratio on the natural convection in a rectangular porous medium" Mansoura Engineering Journal (MEJ), vol 15, No. 1, pp M95-M107, 1990.
  16. Patankar, S., "Numerical Heat transfer and fluid flow" Mc Graw Hill, New York, 1980.
  17. Kim, S., and Vafia, K., "Analysis of natural convection about a vertical plate embedded in a porous medium" Int. J. of Heat and Mass Transfer, vol. 32, No. 4, pp 665-677, 1989.

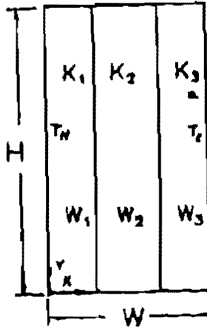


Fig. 1 Schematic diagram of the rectangular multilayered porous cavity.

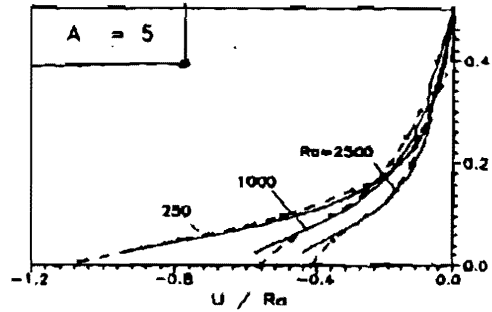


Fig. 2 The horizontal velocity  $U/Ra$  at the middle vertical plane  $X = 0.5$   
 - - - Lauriat and Prasad [12]  
 — Present work

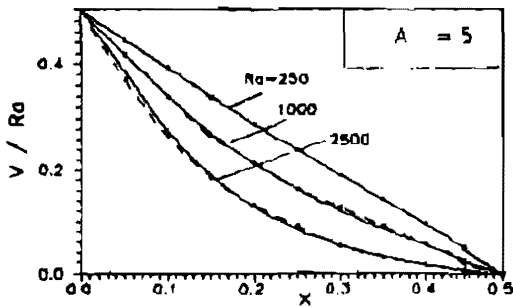


Fig. 3 The Vertical velocity  $V/Ra$  and the non-dimensional temperature  $\theta$  at the midheight section where  $Y = 0.5$   
 - - - Lauriat and Prasad [12], — Present work

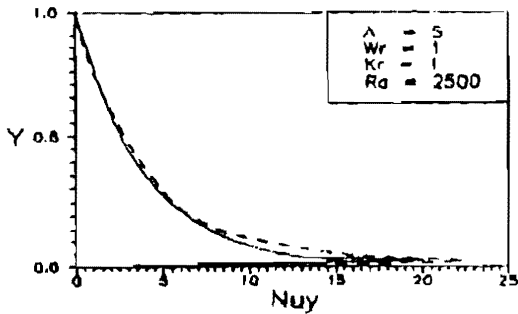
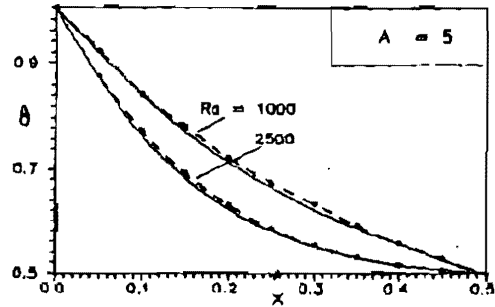


Fig. 4 The local heat transfer rate along the hot wall  
 - - - Lauriat and Prasad [12]  
 — Present work

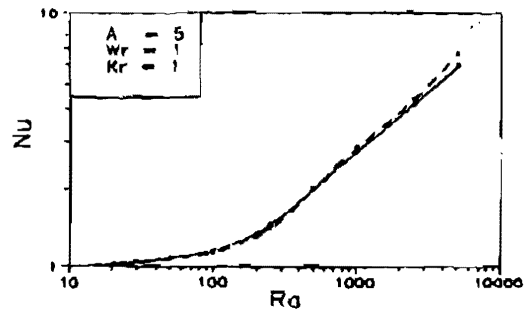


Fig. 5 The average heat transfer rate along the hot wall  
 - - - Lauriat and Prasad [12]  
 — Present work

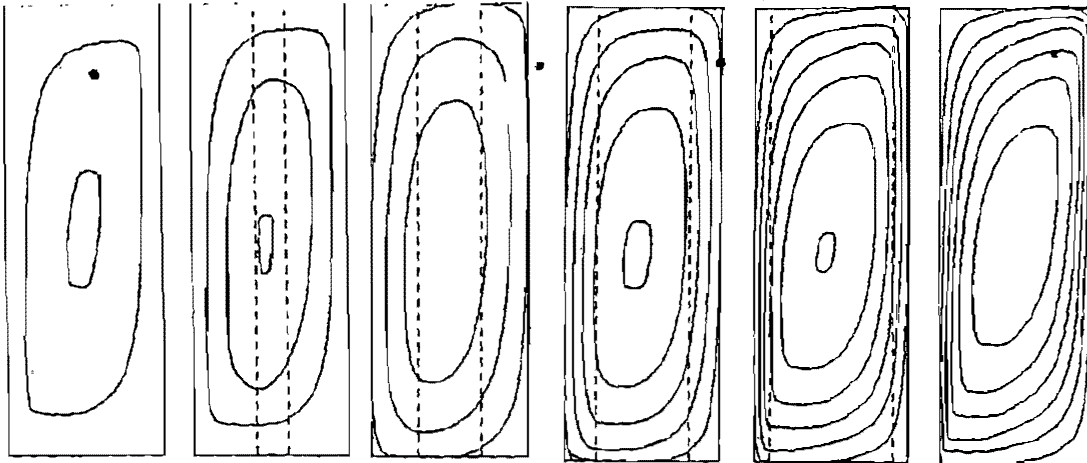


Fig. 6. Streamlines for  $A=3$ ,  $Kr = 5$  and  $Ra = 150$   
 ( $\psi_1 = 8$ ,  $\Delta\psi = 8$ ).

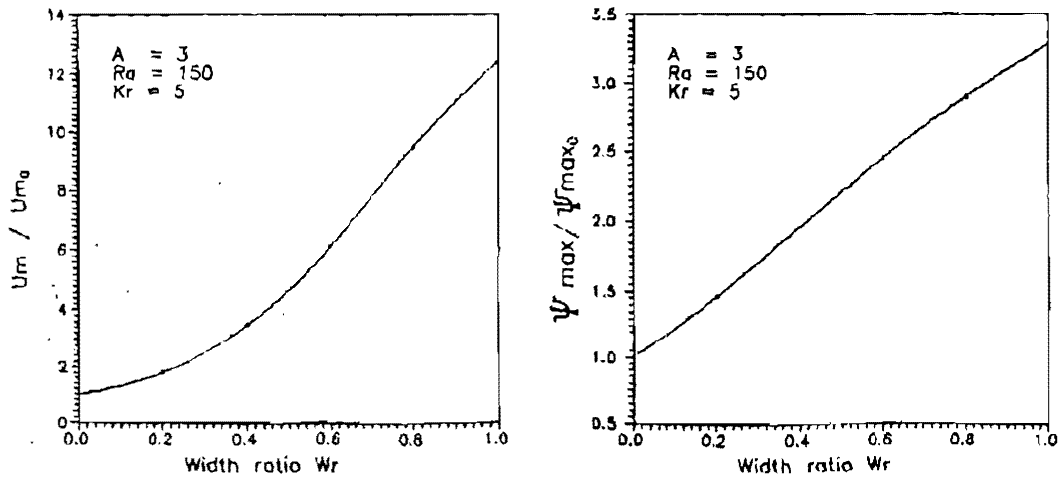


Fig. 7 Variation of the nondimensional average velocity and Streamfunction with the width ratio of the inner sublayer for  $A = 3$ ,  $Kr = 5$  and  $Ra = 150$

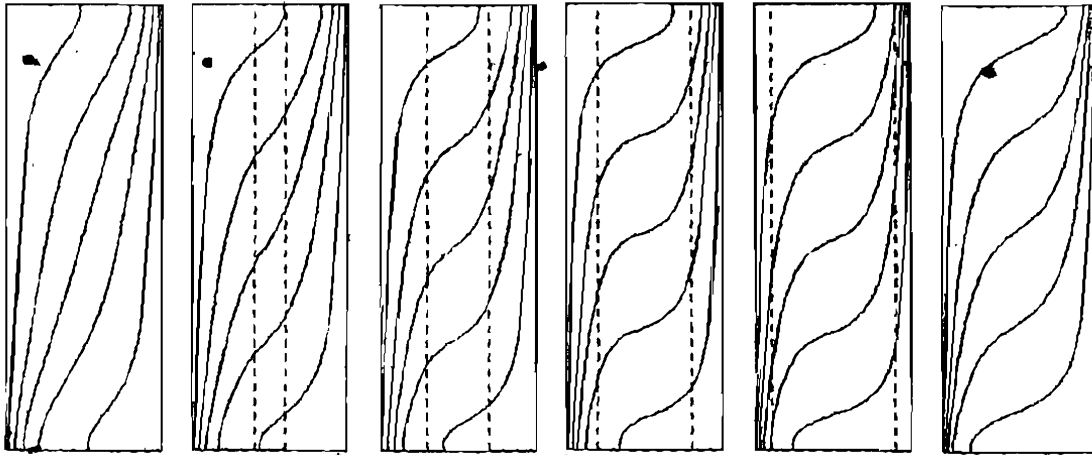


Fig. 8 isotherms for  $A=3$ ,  $Kr = 5$  and  $Ra = 150$   
 ( $\theta_1 = 0.1$ ,  $\Delta\theta = 0.2$ )

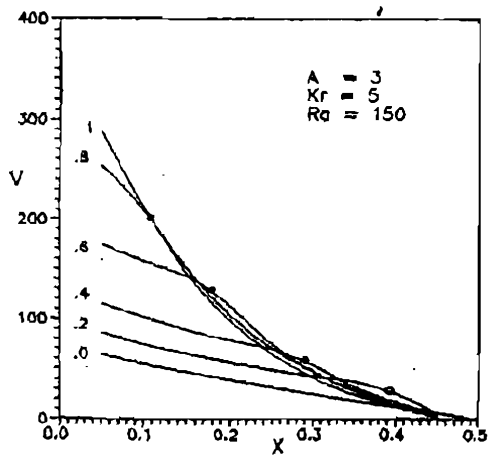
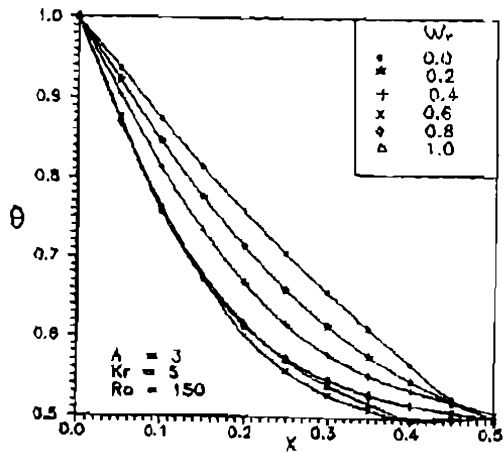


Fig. 9 The effect of the inner sublayer width ratio  $W_s$  on the temperature and velocity distributions at the midheight section where  $Y=0.5$  for  $A=3$ ,  $Kr=5$  and  $Ra=150$ .



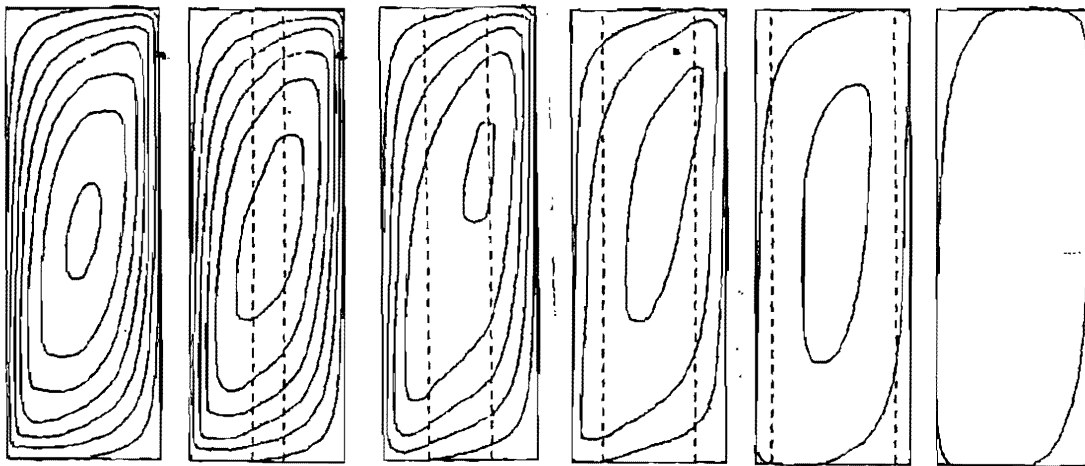


Fig. 10 Streamlines for  $A = 3$ ,  $Kr = 0.2$  and  $Ra = 400$   
 ( $\psi_1 = 5$ ,  $\Delta\psi = 5$ )

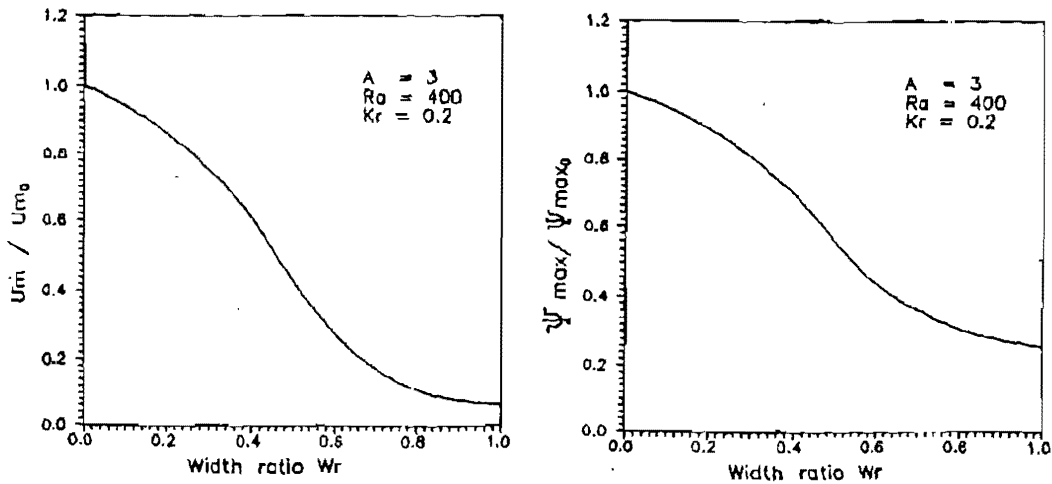


Fig. 11 Variation of the nondimensional average velocity and Streamfunction with the width ratio of the inner sublayer for  $A = 3$ ,  $Kr = 0.2$  and  $Ra = 400$

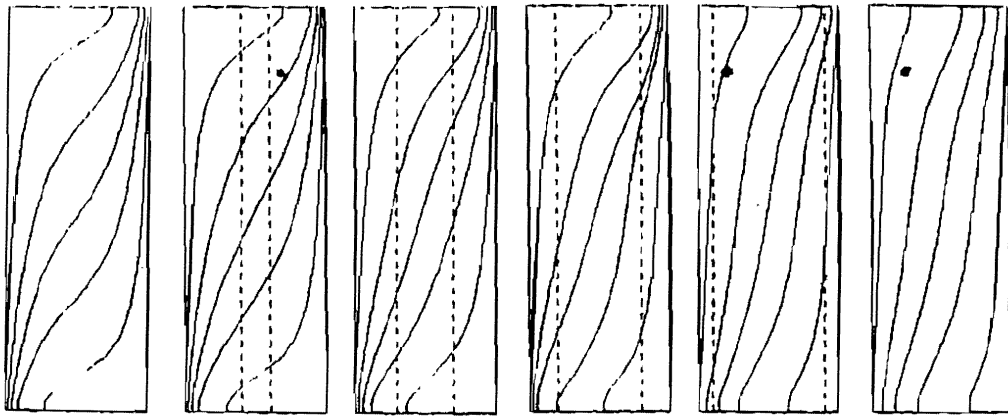


Fig. 12 isotherms for  $A = 3$ ,  $K_r = 0.2$  and  $Ra = 400$   
( $\theta_1 = 0.1$ ,  $\Delta\theta = 0.2$ )

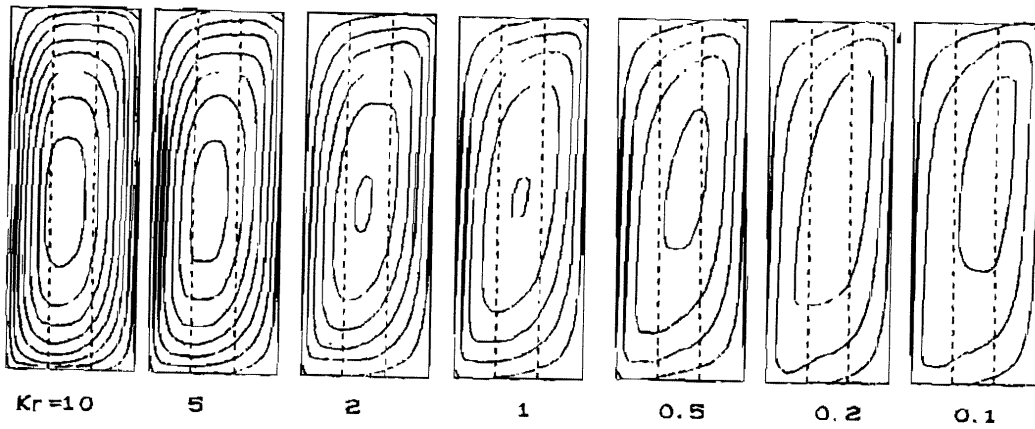


Fig. 13 Streamlines for  $A = 3$ ,  $W_r = 0.333$  and  $Ra = 250$   
( $\psi_1 = 5$ ,  $\Delta\psi = 5$ )

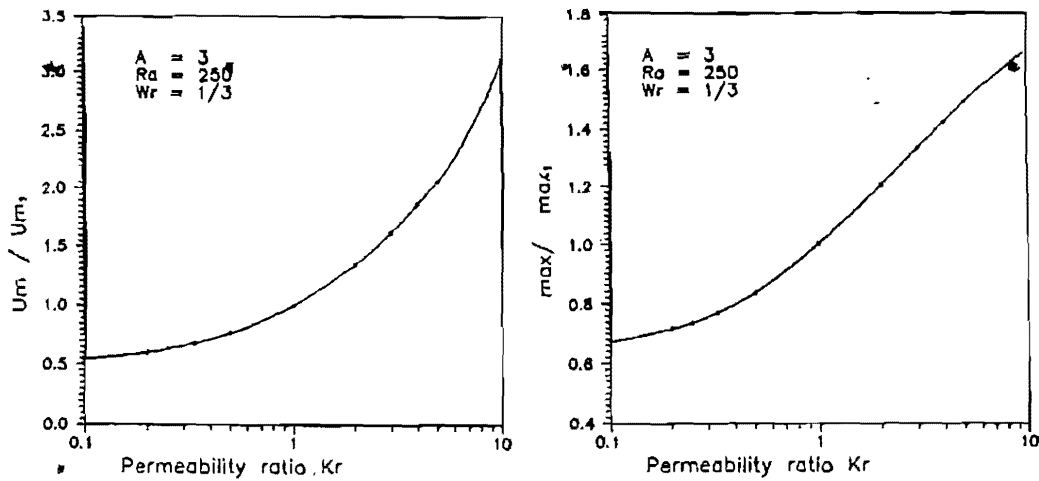


Fig. 14 Variation of the nondimensional average velocity and Streamfunction with the permeability ratio of the inner sublayer for  $A = 3$ ,  $Wr = 1/3$  and  $Ra = 250$

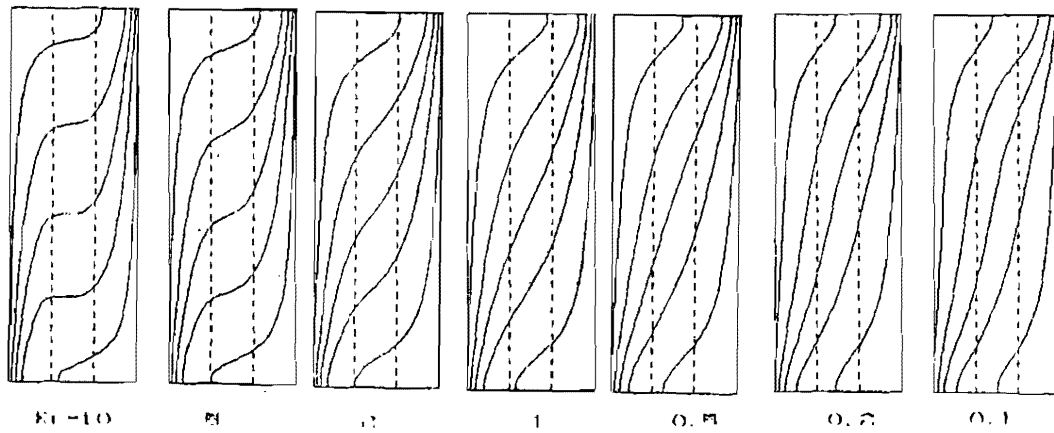


Fig. 15 isotherms for  $A = 3$ ,  $Wr = 1/3$  and  $Ra = 250$  ( $\theta_1 = 0.1, \Delta\theta = 0.2$ )

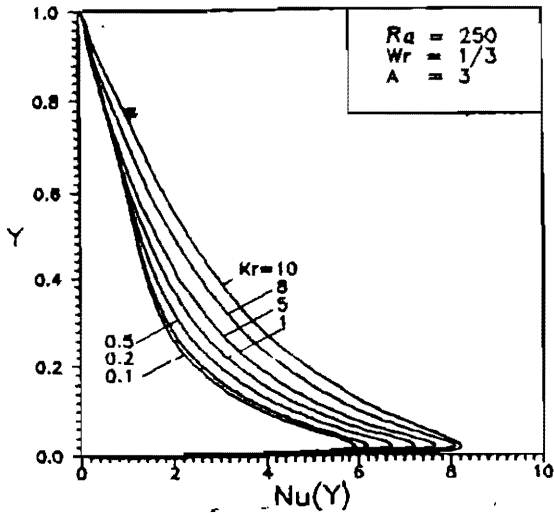


Fig. 16 Effect of the permeability ratio of the inner sublayer  $Kr$  on the local  $Nu$  at the hot wall

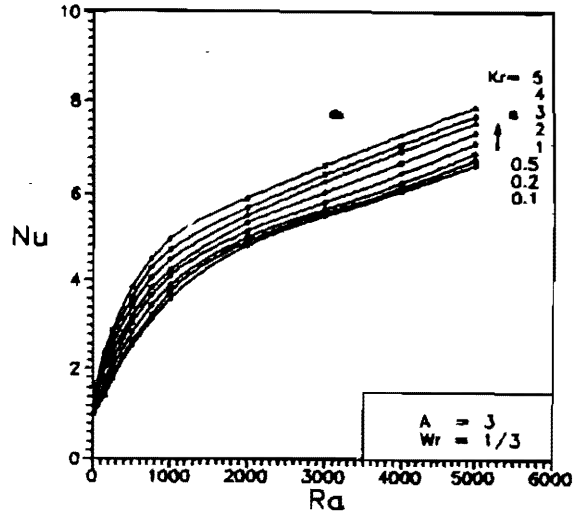


Fig. 17 Effect of the permeability ratio of the inner sublayer  $Kr$  on the average  $Nu$  at the hot wall

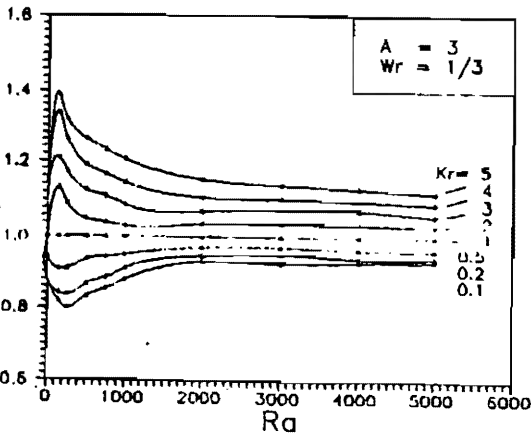


Fig. 18 Effect of the permeability ratio of the inner sublayer on the behavior of  $Nu/Nu_i$  at the hot wall

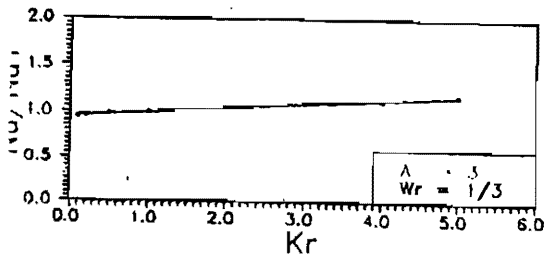


Fig. 19 The behavior of  $Nu/Nu_i$  at the hot wall with the permeability ratio of the inner sublayer in the boundary layer regime

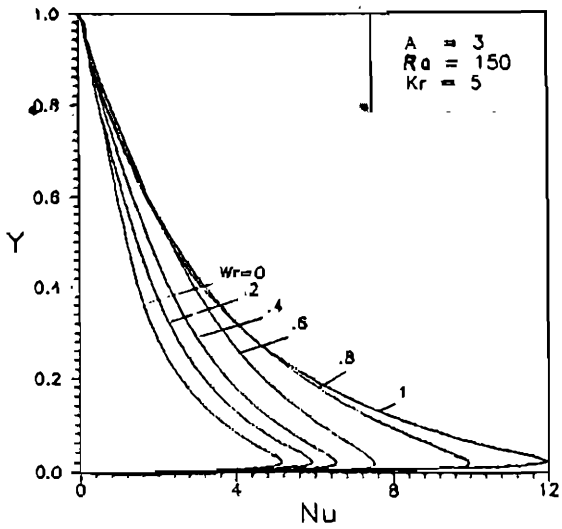


Fig. 20 The local heat transfer rate at the hot wall for  $Kr=5$  and  $Ra=150$

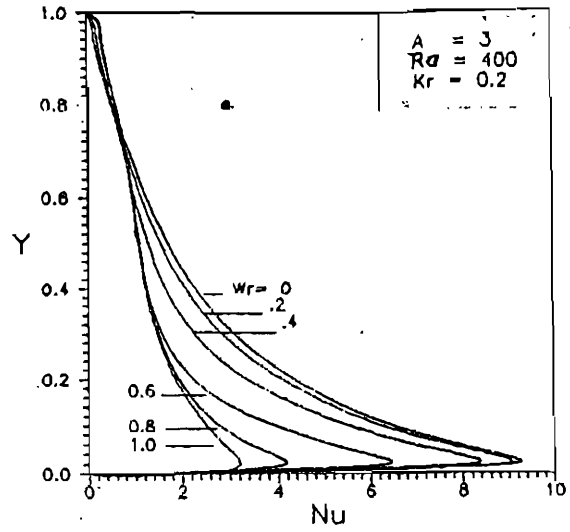


Fig. 21 The local heat transfer rate at the hot wall for  $Kr=0.2$  and  $Ra=150$

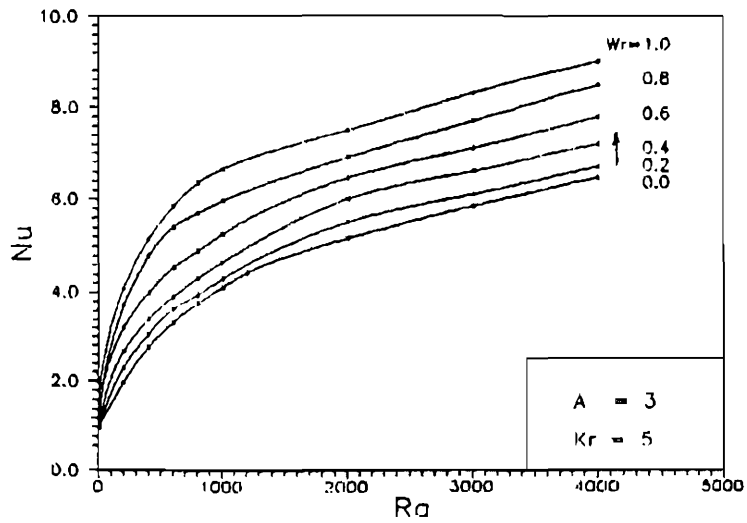


Fig. 22 Effect of the Width ratio of the inner sublayer  $Wr$  on the average  $Nu$  at the hot wall for  $Kr=5$

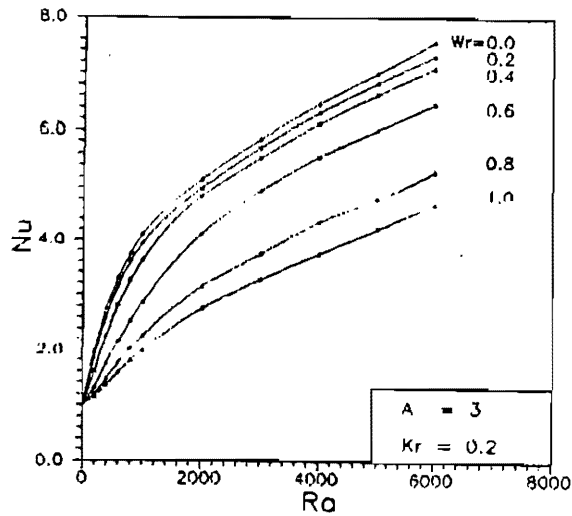


Fig. 23 Effect of the Width ratio of the inner sublayer  $Wr$  on the average  $Nu$  at the hot wall for  $Kr=0.2$

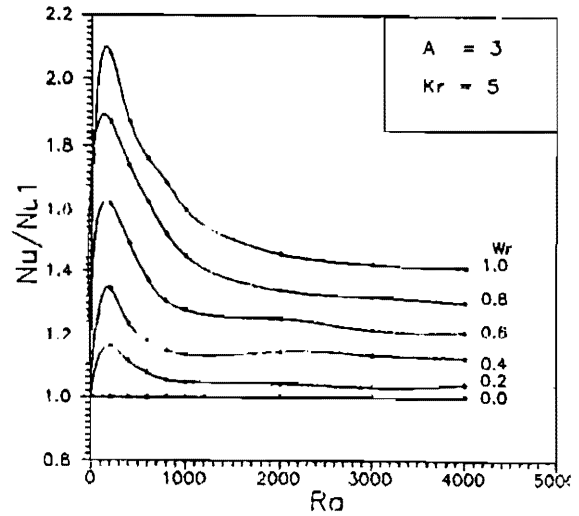


Fig. 24 Effect of the Width ratio of the inner sublayer  $Wr$  on  $Nu/Nu_1$  at the hot wall for  $Kr = 5$

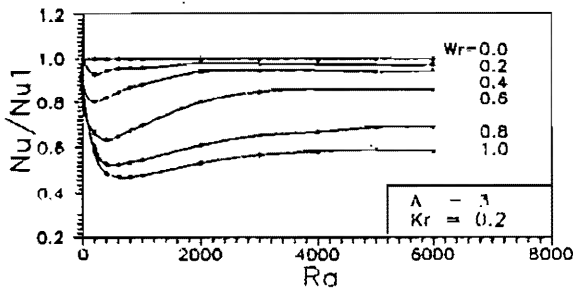


Fig. 25 Effect of the Width ratio of the inner sublayer  $Wr$  on  $Nu/Nu_1$  at the hot wall for  $Kr = 0.2$

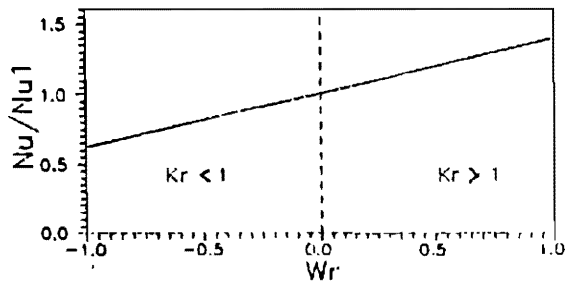


Fig. 26 The behavior of  $Nu/Nu_1$  at the hot wall with the Width ratio of the inner sublayer in the boundary layer regime